Earth and Planetary Science Letters, 96 (1990) 287–304
Elsevier Science Publishers B.V., Amsterdam – Printed in The Netherlands

[KT]

Boundary scavenging in the Pacific Ocean: a comparison of ^{10}Be and ^{231}Pa

R.F. Anderson [1], Y. Lao [1], W.S. Broecker [1], S.E. Trumbore [2,*], H.J. Hofmann [2] and W. Wolfli [2]

[1] *Lamont-Doherty Geological Observatory of Columbia University, Palisades, NY 10964 (U.S.A.)*
[2] *Institut für Mittelenergiephysik, ETH-Honggerberg, CH-8095 Zurich (Switzerland)*

Received May 31, 1989; revised version received October 12, 1989

Concentrations of U, Th, ^{231}Pa and ^{10}Be were measured in Holocene sediments from two cores collected off the west coast of South America, two cores from the East Pacific Rise, two from the equatorial Pacific and one from the south Pacific central gyre. Our results, together with data from 5 cores reported in the literature, show that boundary scavenging plays a major role in the removal of ^{10}Be from the Pacific Ocean. Deposition rates of ^{10}Be at three margin sites are more than an order of magnitude greater than at sites of red clay accumulation in the deep central Pacific. Deposition of ^{231}Pa is 4 to 5-fold greater at the margin sites. The residence time of ^{10}Be with respect to chemical scavenging, defined as its inventory in the water column divided by its rate of removal to the sediments, varies regionally from >1000 years at the red-clay sites in the deep central Pacific to ~ 100 years at the margin sites. Different factors control boundary scavenging of Pa and Be. For example, scavenging of ^{231}Pa is enhanced by metal-oxide coatings of particles, whereas this seems to have little influence on the scavenging of ^{10}Be.

1. Introduction

Several studies have shown that certain insoluble elements are removed from seawater and deposited in sediments at ocean margins at much greater rates than they are deposited in open-ocean sediments. This preferential deposition of insoluble elements at ocean margins has been termed "boundary scavenging" [1], and has been most intensively studied with respect to its effect on the transport and fate of naturally-occurring uranium-series radionuclides such as ^{210}Pb [1–4] and ^{231}Pa [5–8]. Enhanced deposition of fallout-derived Pu isotopes in ocean-margin sediments has also been reported [9–11].

Studies of ^{230}Th and ^{231}Pa have provided the most unequivocal evidence for the existence, and importance, of boundary scavenging. ^{230}Th and ^{231}Pa are introduced into seawater by decay of their respective dissolved uranium progenitors (^{234}U, ^{235}U; the only significant source of ^{230}Th and ^{231}Pa in the oceans) with an initial ^{231}Pa/^{230}Th activity ratio of 0.093. Thorium and protactinium are both very insoluble, being removed to the sediments by chemical scavenging processes on a time scale (10–100 years [5,6]) much less than their radioactive half lives (^{230}Th = 75,200 y; ^{231}Pa = 32,500 y). Since decay in the water column is negligible, the ocean-wide average unsupported ^{231}Pa/^{230}Th activity ratio for newly-formed sediment must equal the production ratio of 0.093. Deviations from a ratio of 0.093 in recent sediments reflect a net lateral redistribution of ^{231}Pa relative to ^{230}Th in the water column during the time interval between their production and burial [5–8,12,13].

^{230}Th is deposited at a relatively uniform rate over the sea floor (when normalized to a constant water depth), with little net lateral transport between its production in the water column and burial in marine sediments [7,12–15]. In contrast to ^{230}Th, ^{231}Pa is extensively redistributed. Examination of ^{231}Pa/^{230}Th ratios in particulate matter and sediments showed that only about 1/3 of the ^{231}Pa produced in central ocean gyres is removed to underlying sediments, with the remaining $\sim 2/3$ being transported to ocean margins prior to burial [5,6,12,13,15]. This net lateral transport occurs over distances of up to thousands of kilometers on time scales of $\leqslant 100$

* Present address: Center for Accelerator Mass Spectrometry, Lawrence Livermore National laboratory, L-397, Livermore, CA 94550, U.S.A.

0012-821X/90/$03.50

years [5,6]. Most elements have residence times in the deep ocean > 100 years, so the potential for boundary scavenging to play an important role in their transport and fate in the ocean is not limited by the length of time required for the elements to be transported laterally over basin-scale distances.

The biogeochemical processes that lead to boundary scavenging, and their relative importance, have not been unambiguously defined. Greater total fluxes of particulate matter near ocean margins certainly contribute to enhanced chemical scavenging. The relative time scales of lateral mixing and of the residence times of the scavenged elements is another important factor [12]. It has also been suggested that specific particulate phases such as MnO_2 coating on particles [1,6] or biogenic opal [15], contribute to enhanced scavenging in ocean-margin waters. However, further work is needed to fully understand the importance of individual particulate phases. Until then, it is impossible to predict from fundamental principles the extent to which a particular element will be affected by boundary scavenging. For now, this must be determined empirically by measuring the deposition rate of an element of interest in representative open-ocean and ocean-margin environments.

^{10}Be is an important tracer for dating deep-sea sediments and Mn nodules [16–18]. A thorough understanding of the sources, transport, and fate of ^{10}Be in the oceans is essential to obtain reliable chronologies from ^{10}Be and to fully utilize it as a tracer of geochemical process. This need for a better understanding of the marine geochemistry of ^{10}Be led us to investigate the extent to which ^{10}Be is preferentially removed from seawater at ocean margins.

Limited evidence suggests that ^{10}Be removal from the oceans may be influenced by boundary scavenging. ^{10}Be accumulation rates in margin sediments off Northwest Africa [19] and off California [20] have been found to be greater than the rate of ^{10}Be supply to the earth's surface from the atmosphere. However, this alone does not unequivocally prove that ^{10}Be is preferentially removed at ocean margins because other physical transport processes, such as sediment focussing by bottom currents and gravity flows (e.g., turbidites, slumps), could also lead to local rates of ^{10}Be accumulation much greater than the ocean-wide average. Some method is needed to correct for the effects of local sediment transport and compare the rates of ^{10}Be scavenging from the water column at ocean-margin and open-ocean sites. Our solution to this problem is to normalize ^{10}Be concentrations in sediments to activities of unsupported ^{230}Th. Bacon and coworkers [21–23] have shown that concentrations of trace elements, $CaCO_3$, clay, etc., can be normalized to ^{230}Th activities to determine regional scavenging rates (fluxes) for the elements (phases) of interest. The relatively uniform deposition of ^{230}Th makes it an ideal tracer against which the concentrations of other elements such as ^{10}Be can be normalized to determine whether or not they are preferentially removed at ocean margins.

The residence time of Be in the deep sea is long enough for lateral mixing to produce a nearly constant ^{10}Be concentration of deep waters within an ocean basin [24], although interocean differences in the concentration of ^{10}Be have been reported [25]. The uniform concentration of ^{10}Be within the deep waters of an ocean basin can, in effect, be treated as a uniform source for chemical scavenging, much like the uniform production of ^{230}Th and ^{231}Pa by U decay. Therefore, ^{10}Be/^{230}Th ratios in marine sediments will reflect the extent to which ^{10}Be is preferentially removed from seawater at ocean margins. This is essentially the same approach that was used to identify boundary scavenging of ^{231}Pa [5–8].

2. Sample locations

^{230}Th, ^{231}Pa and ^{10}Be concentrations were measured in Holocene sediments from several sites representing open-ocean and ocean-margin environments in the Pacific Ocean (Table 1). Sites were selected to examine the effect on boundary scavenging of particle composition, as well as the magnitude of particle flux. RC11-210 and V28-238 are from equatorial areas with relatively high fluxes, for open-ocean regions, of biogenic particles. V18-299 is from the south central Pacific, representing an area more typical of central ocean gyres having a lower particle flux. Although particulate matter fluxes have not been measured near V18-299, studies have shown that primary productivity and the ensuing particle flux are higher at the equator than in central ocean gyre

regions. For example, Betzer et al. [26] measured primary production and particle flux along a N–S transect across the equator at 153° W and showed that primary productivity and particle flux were about four times higher at the equator than at 12° N. Similarly, comparing fluxes measured at MANOP Site C (01°03′N; 138°56′W [27]) and at PARFLUX P_1 (15°21′N; 151°29′W [28]) shows about fourfold higher fluxes of total particulate matter and of organic carbon near the equator (1° N). If the pattern of poleward decrease in particle flux is symmetrical about the equator, then the particle flux near V18-299 would be approximately a quarter of that near RC11-210 and V28-238.

It has been suggested that the presence of manganese (and possibly iron) oxide coatings on particulate matter contributes to enhanced scavenging in ocean-margin regions [1,6]. We have analyzed sediments from two cores collected on the East Pacific Rise (TT154-10 and V19-55) which are known to be rich in Fe and Mn oxyhydroxides derived from venting of metal-rich hydrothermal solutions at the ridge crest [29,30]. Two cores from the equatorial Pacific off Equador (V19-28 and V19-29) were selected to represent an ocean-margin environment.

3. Methods

Prior to dissolution of the samples (about 1–2 g), 1.88 mg of ^{9}Be (as $BeSO_4$ solution) was added as a chemical yield monitor along with ^{236}U, ^{229}Th and ^{233}Pa. Measurement of U, Th and Pa followed approximately the method described before [31]. Following the separation of U, Th and Pa, Be remained with Al and other major elements in a small volume (15–20 ml) of dilute HCl. Be was then purified as follows.

Ten normal NaOH was added to the HCl solution to bring the pH up to 14, which precipitated Mn and residual Fe. After centrifugation, the supernate (containing Al and Be) was decanted and saved. The precipitate was resuspended in a NaOH solution (pH = 14) and centrifuged. The two supernate fractions were combined and then acidified with HCl to pH = 1. Al and Be hydroxides were precipitated overnight by adding NH_4OH to pH between 8 and 9.

The precipitate containing Al and Be was separated from the supernate by centrifugation and then was dissolved by 20 ml 1.2*N* HCl and loaded to a 20 cm column (i.d. 1 cm) of cation exchange resin (Dowex Ag 50W × 12) preconditioned in 1.2*N* HCl. The column was washed with 20 ml of

TABLE 1

Locations and sediment types of Pacific Ocean cores used in this study

Core	Latitude	Longitude	Water depth (m)	Sediment type	Accumulation rate [a] (cm ka^{-1})
Open-ocean sites					
V18-299	16°07′S	149°40′W	4284	pelagic, carbonate ooze	0.6–0.8
RC11-210	01°49′N	140°03′W	4420	pelagic, carbonate ooze	1.2
V28-238	01°01′N	160°29′E	3120	pelagic, carbonate ooze	1.8
TT154-10	10°17′S	111°20′W	3225	pelagic, rich in metal-oxides	2.4
V19-55	17°00′S	114°11′W	3177	pelagic, rich in metal-oxides	1.2
Ocean-margin sites					
V19-28	02°22′S	84°39′W	2720	hemipelagic	5.4
V19-29	03°35′S	83°56′W	3157	hemipelagic	10.0

[a] Average Holocene accumulation rates of the cores are from the following sources: Radiocarbon (AMS) ages of TT154-10 and V28-238 are from [67]. The chronostratigraphy of RC11-210 is based on the $\delta^{18}O$ record of *Globoratalia tumida* [52]. The time scale of V19-28 is from a reinterpretation of the $\delta^{18}O$ record by Lyle et al. [51]. For V18-55 and V19-29, the core depths of the last glacial maximum (18 ka B.P.) were given by Moore et al. [68]. The ages of the samples in these two cores are derived assuming constant sediment accumulation rates since 18 ka B.P. For V18-299, we measured downcore U-series isotopes and used the excess ^{230}Th and ^{231}Pa to construct the sediment accumulation rate of the core. $\delta^{18}O$ of the bulk carbonate was also measured from which the 18 ka horizon was assigned to a depth of 16 cm. The lower accumulation rate is the long term average based on U-series results while the higher value is obtained by assuming constant accumulation since 18 ka.

TABLE 2

Measured isotope concentrations and ratios for deep Pacific Ocean sediments

Core, depth (cm)	Concentration (dpm g^{-1})				^{10}Be (10^9 at g^{-1})	Activity ratio	
	^{238}U	^{232}Th	^{230}Th	^{231}Pa		$^{238}U/^{232}Th$	$^{230}Th/^{232}Th$
V18-299							
0–5	0.98±0.04	1.164±0.035	72.10±1.02	2.93±0.15	9.56±0.32	0.84± 0.04	62± 2
RC11-210							
5–7	0.17±0.01	0.090±0.005	22.65±0.31	1.45±0.04	2.98±0.10	1.89± 0.85	250± 13
V28-238							
0–8	0.19±0.01	0.137±0.007	8.98±0.14	0.56±0.03	1.18±0.05	1.39± 0.10	66± 3
14–16	0.18±0.01	0.142±0.008	8.20±0.13	0.45±0.02	1.27±0.04	1.27± 0.11	58± 3
TT154-10							
1.2–2.4	0.47±0.02	0.020±0.003	13.78±0.20	1.93±0.07	2.65±0.09	23.5 ± 3.7	702±114
4.2–6.0	0.48±0.02	0.015±0.004	13.42±0.22	2.01±0.06	2.28±0.06	32.0 ± 8.6	925±257
V19-55							
0–2	1.32±0.06	0.022±0.005	20.79±0.35	2.84±0.10	4.15±0.12	60 ±14	942±212
8–10	1.56±0.06	0.032±0.004	19.32±0.30	2.45±0.08	3.99±0.11	48.8 ± 6.4	597± 74
V19-28							
17–19	1.48±0.06	0.192±0.010	5.18±0.12	0.94±0.03	3.16±0.09	7.71± 0.51	27± 1
57–59	2.56±0.09	0.126±0.008	3.93±0.11	0.64±0.03	2.74±0.07	20.3 ± 1.5	31± 2
V19-29							
17–19	1.56±0.06	0.511±0.023	6.38±0.15	1.08±0.05	5.35±0.13	3.05± 0.18	13± 1
45–47	5.39±0.19	0.414±0.021	5.38±0.13	0.82±0.04	4.19±0.11	13.0 ± 0.8	13± 1

1.2*N* HCl and eluant was discarded. Be was eluted from the column with an additional 50 ml of 1.2*N* HCl. A clean teflon beaker (250 ml) was used to collect Be which was ready for solvent extraction. If the sample was carbonate rich, i.e., low Al content, then the above coprecipitation and cation exchange steps were omitted, and Be purification began with the following solvent extraction.

To the 50 ml Be solution was added 6 ml of Na_2EDTA solution (20g Na_2EDTA + 110 ml 1*N* NH_4OH) and a magnetic stir bar. The pH was raised to 6 with NH_4OH and then 6 ml of acetyl acetone was added. The mixture was stirred for 2 hours, after which 20 ml of chloroform ($CHCl_3$) was added to the solution and stirring continued for about 20 minutes. Then the solution was transferred to a teflon separatory funnel and shaken for 5 minutes. After the phases separated, the $CHCl_3$ phase (containing Be) was drained into a clean teflon beaker. The aqueous phase in the separatory funnel was further extracted with an additional 10 ml of $CHCl_3$. The two fractions of $CHCl_3$ (30 ml) were combined and transferred to a clean teflon separatory funnel and 10 ml of 7*N* HCl was added and shaken for 5 minutes. The $CHCl_3$ was drained into the used beaker and the HCl (containing Be) into a clean teflon beaker. The $CHCl_3$ was returned to the separatory funnel and extracted with additional 10 ml of 7*N* HCl. The combined HCl solution was heated to dryness 3 times in conc. HNO_3. Then conc. HCl was added and heated to dryness 2 times.

The residue was dissolved in 10 ml of 0.12*N* HCl and loaded to a second cation column which was identical to the first one except that the cation exchange resin was conditioned in 0.12*N* HCl. The column was first washed with 30 ml of 0.12*N* HCl and then 35 ml of 1.2*N* HCl and all the eluant up to this point was discarded. 50 ml of 1.2*N* HCl was used to elute Be out of column (residual Al remained in the resin). The Be solution was collected in a clean teflon beaker and heated. When near dryness, 1 ml of conc. HNO_3 was added and then evaporated to dryness. The residue was taken up with 2 ml of conc. HCl and then evaporated to 0.5 ml. 5 ml of Milli-Q H_2O was added to the 0.5 ml HCl solution and heated gently for a few minutes. NH_4OH was added to precipitate $Be(OH)_2$ at pH = 8 ~ 10 overnight. The precipitate was filtered onto an ashless combustible filter (Whatman #42) and combusted in a Pt crucible at 900°C for 4 hours. The Be oxide was

then analyzed by accelerator mass spectrometer [32].

4. Results and discussion

Measured ^{230}Th and ^{231}Pa activities (Table 2) consist of three components: that which was scavenged from seawater, the principal component of interest, that which was supported by U in the detrital minerals, and that which was produced by decay of authigenic U found in the sediments. Authigenic U is present in most of the sediments analyzed, as can be seen by comparing activities of ^{238}U with those of ^{232}Th. Lithogenic material has a $^{238}U/^{232}Th$ activity ratio of about unity, reflecting the average crustal abundances of U and Th [33]. Organic-rich margin sediments (V19-28 and V19-29) and metalliferous sediments from the East Pacific Rise (TT154-10 and V19-55) both have $^{238}U/^{232}Th$ activity ratios greatly in excess of one (Table 2). This authigenic uranium must be taken into account in calculating unsupported ^{230}Th and ^{231}Pa activities. Based on surveys of the literature, and on other work done in our laboratory, an average $^{238}U/^{232}Th$ activity ratio for the lithogenic fraction of marine sediments is estimated to be 0.8 ± 0.2. This factor was used along with the measured ^{232}Th activity to correct for the lithogenic component (i.e., the detrital U-supported fraction) of ^{230}Th and ^{231}Pa. It was further assumed that authigenic uranium accumulation was synchronous with deposition of the sediments, so simple ingrowth equations could be used to evaluate the production of ^{230}Th and ^{231}Pa by decay of authigenic U. The component of ^{230}Th scavenged from seawater, hereafter referred to as the unsupported fraction, was then calculated as:

$$
\begin{aligned}
{}_{xs}{}^{230}\mathrm{Th} = {}^{230}\mathrm{Th}_m &- (0.8 \pm 0.2)^{232}\mathrm{Th}_m \\
&- 1.14\left[{}^{238}\mathrm{U}_m - (0.8 \pm 0.2)^{232}\mathrm{Th}_m\right] \\
&\cdot \left[1 - \exp(-\lambda_{230} t)\right] \qquad (1)
\end{aligned}
$$

TABLE 3

Initial isotope concentrations, ratios, and deposition indices for ^{231}Pa and ^{10}Be

Core, depth (cm)	Age [a] (ka)	$_{xs}{}^{230}\mathrm{Th}_0$ [b] (dpm/g)	$_{xs}{}^{231}\mathrm{Pa}_0$ [b] (dpm/g)	$_{xs}(^{231}\mathrm{Pa}/^{230}\mathrm{Th})_0$ (activity ratio)	^{231}Pa deposition index [c]	$^{10}\mathrm{Be}/_{xs}{}^{230}\mathrm{Th}_0$ (10^9 at/dpm)	^{10}Be deposition index [c]
V18-299							
0–5	6.0	75.21 ± 1.10	3.32 ± 0.17	0.044 ± 0.002	0.48 ± 0.02	0.127 ± 0.004	1.04
RC11-210							
5–7	6.0	23.85 ± 0.33	1.64 ± 0.07	0.069 ± 0.002	0.75 ± 0.02	0.125 ± 0.004	1.02
V28-238							
0–8	4.8	9.27 ± 0.15	0.62 ± 0.03	0.067 ± 0.003	0.72 ± 0.03	0.127 ± 0.005	1.04
14–16	8.5	8.74 ± 0.14	0.54 ± 0.02	0.062 ± 0.003	0.67 ± 0.03	0.145 ± 0.006	1.19
TT154-10							
1.2–2.4	5.9	14.50 ± 0.21	2.19 ± 0.08	0.151 ± 0.006	1.63 ± 0.06	0.183 ± 0.007	1.50
4.2–6.0	6.8	14.24 ± 0.24	2.32 ± 0.06	0.163 ± 0.005	1.76 ± 0.06	0.160 ± 0.005	1.31
V19-55							
0–2	5.1	21.32 ± 0.30	3.15 ± 0.11	0.148 ± 0.005	1.60 ± 0.06	0.195 ± 0.006	1.60
8–10	7.7	20.58 ± 0.32	2.86 ± 0.10	0.139 ± 0.005	1.50 ± 0.06	0.194 ± 0.006	1.59
V19-28							
17–19	5.3	5.21 ± 0.14	1.04 ± 0.04	0.200 ± 0.009	2.16 ± 0.10	0.607 ± 0.024	4.98
57–59	10.5	3.93 ± 0.12	0.77 ± 0.03	0.197 ± 0.010	2.13 ± 0.11	0.699 ± 0.027	5.73
V19-29							
17–19	1.8	6.05 ± 0.18	1.12 ± 0.05	0.186 ± 0.010	2.01 ± 0.11	0.884 ± 0.034	7.25
45–47	4.5	5.03 ± 0.16	0.88 ± 0.05	0.175 ± 0.010	1.89 ± 0.11	0.833 ± 0.034	6.83

[a] Sources for sediment chronologies are given in Table 1.

[b] Subscript "xs" designates unsupported value. Subscript "0" indicates that the measured activities of xs (unsupported) ^{230}Th and ^{231}Pa have been decay corrected to the time at which the sediments were deposited.

[c] Deposition Indices represent the measured $(N/_{xs}{}^{230}\mathrm{Th})_0$ ratio, where $N = {}^{231}\mathrm{Pa}$ or ^{10}Be, divided by the ocean-wide average value for the ratio. Values < 1.0 indicate net loss of N by lateral transport while values > 1.0 reflect a net lateral import of the isotope relative to ^{230}Th. See text.

and for ^{231}Pa:

$$_{xs}{}^{231}Pa = {}^{231}Pa_m - 0.046(0.8 \pm 0.2)^{232}Th_m - 0.046\left[{}^{238}U_m - (0.8 \pm 0.2)^{232}Th\right] \cdot \left[1 - \exp(-\lambda_{231} t)\right] \quad (2)$$

where subscripts "xs" and "m" refer to unsupported and measured activities, respectively, t is the time since deposition of the sediments, and λ is the appropriate radioactive decay constant. The factors 1.14 and 0.046 represent the $^{234}U/^{238}U$ and the $^{235}U/^{238}U$ activity ratios in seawater, respectively. Equation (1) fails to correct for decay of unsupported authigenic ^{234}U, but this correction is negligible for the results reported here because all of the samples are of Holocene age.

Uncertainties derived from counting statistics for each nuclide were propagated along with the 25% uncertainty in the lithogenic U/Th ratio to obtain the reported uncertainties for the unsupported ^{230}Th and ^{231}Pa activities. Unsupported ^{230}Th and ^{231}Pa activities at the time of sediment deposition (Table 3) were calculated from the average age of each sample, t, as:

$$_{xs}N_0 = {}_{xs}N \cdot e^{\lambda t} \quad (3)$$

where $_{xs}N$ is the unsupported ^{230}Th or ^{231}Pa activity calculated from equation (1) or (2), respectively. For V28-238 and TT154-10, measured ^{14}C ages were used for t. For the other open-ocean cores, a bioturbated mixed layer of 5 or 6 cm was assumed in assigning an age to surface samples (see Table 1 for sources of core chronologies). Sediment accumulation rates at the margin sites were sufficiently rapid that the effect of bioturbation on the age correction is negligible.

4.1. $^{230}Th/^{232}Th$ ratios in the South Pacific

Before discussing the evidence for boundary scavenging, note that the $^{230}Th/^{232}Th$ ratios of the East Pacific Rise sediments (Table 2; TT154-10 and V19-55)are the highest ever reported for marine samples other than corals. The large uncertainties result from the very small number of ^{232}Th counts detected by alpha spectrometry. Reanalysis of the two samples from TT154-10 by mass spectrometry gave $^{230}Th/^{232}Th$ activity ratios of 790 ± 10 (1.2–2.4 cm) and 800 ± 17 (4.2–6.0 cm), confirming the high ratios obtained by alpha spectrometry. Thorium is not significantly removed from basalts by hydrothermal solutions, and the Th which is injected into seawater from mid-ocean ridge vents has a $^{230}Th/^{232}Th$ activity ratio certainly < 100 and probably < 10 [34,35]. Therefore, seawater is the only reasonable source for Th with a $^{230}Th/^{232}Th$ activity ratio of ~ 800. These high ratios are, in fact, a lower limit for the isotopic composition of Th dissolved in South Pacific deep water because the EPR sediments must contain some lithogenic material, which has a $^{230}Th/^{232}Th$ activity ratio of about unity, as noted above.

Previously reported values for the $^{230}Th/^{232}Th$ ratio of Th dissolved in seawater have generally been less than 200 [5,6,36–40]. Most of these ratios were measured in samples from the North Pacific. $^{230}Th/^{232}Th$ ratios of ~ 800 in EPR sediments indicate one of two things: either the $^{230}Th/^{232}Th$ ratio of Th dissolved in South Pacific deep waters is much greater than in North Pacific waters, or, the North Pacific samples suffered from some form of ^{232}Th contamination. The latter seems unlikely because the North Pacific samples were collected and analyzed by a variety of methods and were processed by investigators in at least 4 different laboratories. It is more likely that the $^{230}Th/^{232}Th$ ratios reflect regional variability in the supply of ^{232}Th to the oceans. The residence time of Th in the deep sea is only 20–40 years [5,6], too short to permit intrabasin homogenization of ^{232}Th concentrations by lateral mixing. Therefore, it is not unreasonable that regional variations in the ^{232}Th content of deep ocean water should exist which reflect a balance between local supply and chemical scavenging.

The East Pacific Rise is situated to receive minimal supply of continental lithogenic material, the leaching of which provides the predominant source of dissolved ^{232}Th in the oceans. Lithogenic material is supplied to the central Pacific primarily by atmospheric transport of continental dust [41]. Eolian transport of dust to the equatorial Pacific is one to two orders of magnitude less than the rate of supply to the central North Pacific gyre at about 38°N [41–43]. The region around the EPR at 10–17°S, where our cores were collected, should therefore have received a substantially lower eolian input of lithogenic dust (i.e., ^{232}Th), than is supplied to regions of the North Pacific

from which previous Th results were obtained. The continental margins are themselves sources of lithogenic particles, and hence ^{232}Th, to the deep sea [40]. The Peru-Chile trench would tend to trap lithogenic material moving downslope from the continent before it reaches the EPR. Furthermore, the EPR rises above the surrounding abyssal plain where fine-grained lithogenic particles could be transported in nepheloid layers. Consequently, there is little opportunity for supply of lithogenic particles to deep waters surrounding the crest of the EPR. This very weak source of ^{232}Th leads to extremely low concentrations of ^{232}Th in deep south Pacific waters which, in turn, are reflected in ^{230}Th/^{232}Th ratios in EPR sediments much higher than in the North Pacific or elsewhere.

4.2. ^{230}Th and ^{231}Pa results in the context of earlier studies

Unsupported ^{231}Pa/^{230}Th ratios measured in this survey are generally consistent with results from earlier work. Results are presented here as Pa/Th ratios, rather than the more traditional Th/Pa ratios, because it is normalization to ^{230}Th that permits lateral transport to be evaluated. ^{231}Pa and ^{230}Th are produced by U decay in seawater at an initial ^{231}Pa/^{230}Th activity ratio of 0.093. Sediments from V18-299, where the lowest particulate flux occurs, have an initial unsupported ^{231}Pa/^{230}Th activity ratio of 0.044 (Table 3) which is even a little high for central ocean gyres [7]. Sediments from V19-28 and V19-29 have ratios of 0.18–0.20, which are typical of ocean margins [6,7]. East Pacific Rise sediments also have ^{231}Pa/^{230}Th ratios (0.14–0.16) greater than the ocean-wide average (0.093), reflecting the enhanced scavenging of Pa from bottom waters by metal oxyhydroxide phases [30]. Enrichment of ^{231}Pa in metalliferous sediments is consistent with the hypothesis that Mn-oxide coatings on particles contribute to the enhanced scavenging of Pa at (some) ocean margins [6].

One new feature of the distribution of ^{230}Th and ^{231}Pa in the Pacific is that ^{231}Pa/^{230}Th ratios in equatorial sediments (0.069 in RC11-210 and 0.062–0.067 in V28-238) are nearly a factor of two greater than ratios typically found in central ocean gyres (often < 0.033 [7]), indicating an enhanced scavenging of Pa from the equatorial Pacific water column. The eolian input of aluminosilicate phases at the equator is one to two orders of magnitude less than the North Pacific central gyre [41–43], and there should not be a significant source of metalliferous particulate phases at these equatorial sites. Something other than lithogenic particles or metal oxide coatings must be responsible for the enhanced scavenging of Pa. Bruland and Coale [44] showed that higher biological productivity at the equator leads to enhanced scavenging of ^{234}Th from surface waters compared to scavenging rates in regions to the north and south. Apparently the relatively greater flux of particles generated by the higher biological productivity in equatorial surface waters also leads to enhanced scavenging throughout the deep water column where virtually all of the ^{230}Th and ^{231}Pa in the sediments originates. Note, however, that the ^{231}Pa/^{230}Th ratios in equatorial sediments are less than the production ratio of 0.093. Although scavenging is enhanced relative to central ocean gyres, there is still a net loss of ^{231}Pa from equatorial Pacific waters by lateral transport to the margins.

4.3. Boundary scavenging of ^{10}Be

Lateral transport of ^{231}Pa was quantified by comparing ^{231}Pa/^{230}Th ratios of sediments and particulate matter from different ocean regions [6,13]. Dividing decay-corrected ^{231}Pa/^{230}Th ratios of sediments by the production ratio of 0.093 produces a simple deposition index, I_D[Pa], which reflects the net lateral import (I_D[Pa] > 1.0) or export (I_D[Pa] < 1.0) of ^{231}Pa at each site examined. A similar deposition index for ^{10}Be can be defined by dividing decay-corrected ^{10}Be/^{230}Th ratios measured at specific sites by the ocean-wide average value for this ratio:

$$I_D[\mathrm{Be}] = (^{10}\mathrm{Be}/\mathrm{xs}^{230}\mathrm{Th})_m/(^{10}\mathrm{Be}/\mathrm{xs}^{230}\mathrm{Th})_{avg} \quad (4)$$

This index is not quite identical to I_D[Pa] because of the different nature of the sources of ^{10}Be and ^{231}Pa, but it is a useful parameter that permits easy visualization of the relative scavenging intensity of ^{10}Be in different ocean regions. For now, we adopt a value of 0.122×10^9 (at dpm^{-1}) for $(^{10}\mathrm{Be}/\mathrm{xs}^{230}\mathrm{Th})_{avg}$, which is obtained by dividing the global ^{10}Be production rate (1.21×10^9 at cm^{-2} ka^{-1} [45]) by the rate of ^{230}Th production in an average 3800 m deep ocean (9.88 dpm cm^{-2} ka^{-1}). Although the value of $(^{10}\mathrm{Be}/\mathrm{xs}^{230}\mathrm{Th})_{avg}$ for the Pacific may be revised when more sedi-

TABLE 4

^{10}Be deposition index values calculated from results reported in the literature

Core site	Latitude	Longitude	Water depth (m)	^{10}Be/xs^{230}Th [a] (10^9 at dpm^{-1})	^{10}Be deposition index [b]	Reference
V28-258	11°52′S	165°45′W	5528	0.061 [c]	0.50	[25]
				0.021 [d]	0.17	[25]
MSN 147G	08°20′N	145°24′W	5110	0.031	0.25	[46]
NOVA III-13	03°56′N	178°47′W	5351	0.065	0.53	[46]
NOVA III-16	00°14′N	179°08′W	5585	0.048	0.39	[46]
MSN 96	57°55′S	157°15′W	4760	0.098	0.80	[46]
DSDP 580	41°38′N	153°59′E	5385	0.52	4.26	[47]
MANOP H	06°32′N	92°50′W	3600	0.24 [e]	1.97	[48,49]
MANOP M	08°50′N	104°W	3100	0.29 [e]	2.38	[48,49]

[a] Decay corrected to time of deposition as described in text.
[b] Calculated according to equation (4) in text.
[c] Measured ratio in core-top sediments.
[d] Ratio obtained by extrapolating profiles to zero depth.
[e] Ratios represent average values for sediment trap samples collected at water depths > 2000 m.

ment data become available, I_D values calculated from our data can still be used to compare the relative rates of ^{10}Be scavenging among these sites.

Deposition index values for ^{231}Pa and ^{10}Be calculated from our data are presented in Table 3. Additional I_D[Be] values calculated from ^{10}Be and ^{230}Th results reported in the literature are listed in Table 4. Ku et al. [25] measured a ^{10}Be/xs^{230}Th ratio of 0.061 (10^9 at dpm^{-1}) in core-top sediments of V28-258 (11°52′S, 165°45′W, 5528 m), about half our open-ocean ratio. Complete ^{10}Be and ^{230}Th profiles were reported for this core. The surface-most ^{230}Th activity, from which the above ^{10}Be/xs^{230}Th ratio was calculated, is below that expected from the trend established by deeper samples. Extrapolating the complete profiles to the surface, which corrects for decay in the mixed layer, produces a (^{10}Be/xs^{230}Th)$_0$ ratio of only 0.021 (10^9 at dpm^{-1}). Both measured and extrapolated ratios are reported in Table 4. ^{10}Be and ^{230}Th results from four red clay cores studied by Amin et al. [46] were decay corrected using their reported values for sediment accumulation rate at each site. A 5 cm thick mixed layer was assumed when decay corrections required a mixed layer thickness. Nuclide activities from DSDP site 580 [47] and MANOP Sites H and M [48,49] were used without decay correction because the former were from rapidly accumulating sediments and the latter from sediment trap samples, neither of which required significant decay corrections.

Amin et al. [46] also calculated the xs^{230}Th inventories for their cores and found that, with one exception, they approximately balanced ^{230}Th production in the overlying water column. This is consistent with other results indicating little lateral redistribution of ^{230}Th in the deep sea. More important, it indicates that recent sediments have not been lost from these sites due to erosion by bottom currents, nor were significant amounts of surface sediments lost during the coring process. Loss of surface sediments under either of these conditions would lead to high apparent values for ^{10}Be/xs^{230}Th$_0$ ratios at these red-clay sites.

Deposition index values for ^{231}Pa and ^{10}Be are summarized in Figs. 1 and 2. Although the number of data points is still relatively small, the patterns of scavenging intensity indicated by these I_D values is consistent with previous results for Th and Pa summarized by Yang et al. [7]. I_D values much less than 1.0, indicating net lateral export, occur at open-ocean sites. I_D values are much greater than 1.0 at the margin sites, indicative of enhanced scavenging which in turn leads to net lateral import of ^{231}Pa and ^{10}Be to these regions.

Enrichment of ^{10}Be in ocean-margin sediments suggests that boundary scavenging plays an important role in the removal of Be from the ocean.

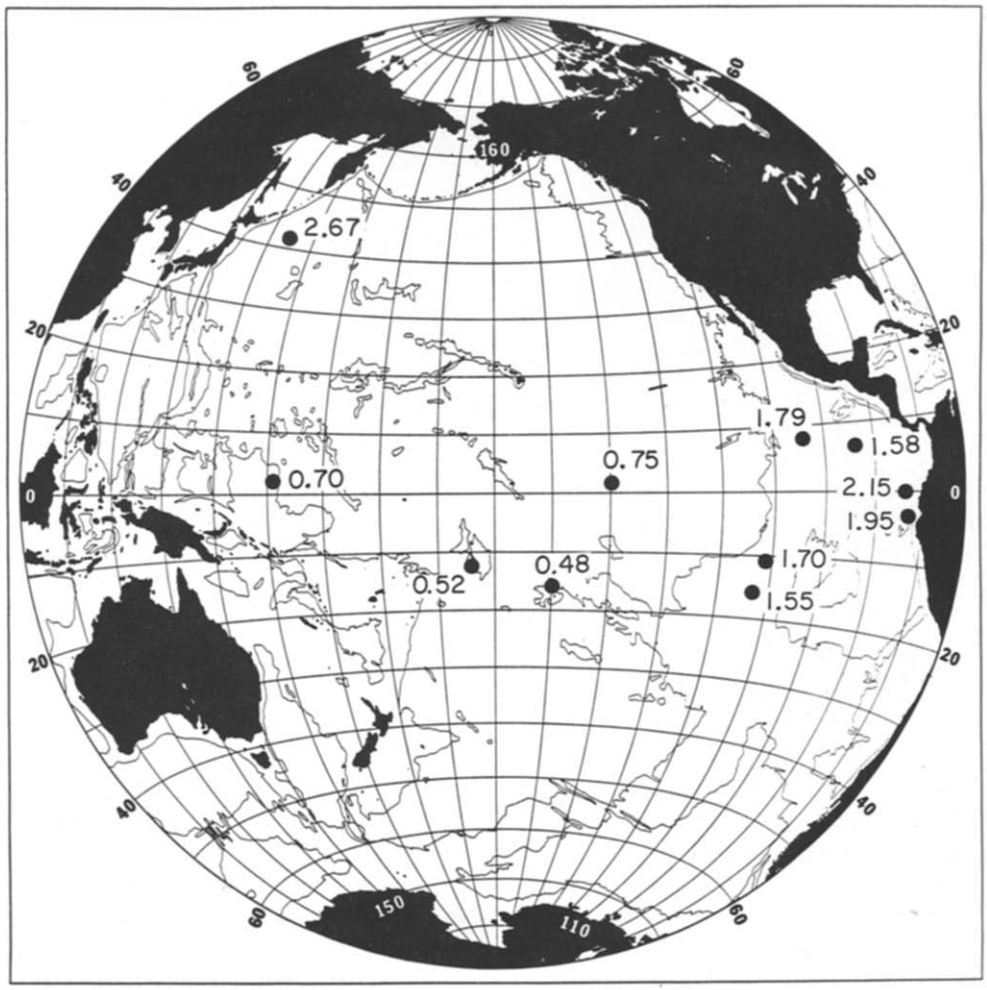

Fig. 1. Deposition Index values for ^{231}Pa. A value less than 1.0 indicates that ^{231}Pa is removed from the water column to the sediments at a rate less than its rate of production in the water column while the converse is true for values greater than 1.0. I_D[Pa] is a measure of the net lateral export or import of Pa at each site. I_D[Pa] values for our cores are from Table 3. I_D[Pa] values for the region around DSDP 580 are calculated from [7]. Values for the MANOP sites are from [49] while Pa and Th data from [72] were used to calculate I_D[Pa] for V28-258.

Another factor to consider before accepting this conclusion is whether or not the excess ^{10}Be in margin sediments could reflect local supply from the continents. The ^{10}Be concentrations of river sediments range world-wide from 1 to 4×10^8 at g^{-1} [50], much too low to have contributed significantly to the ^{10}Be content of the sediments at the two margin sites off South America ($3–5 \times 10^9$ at g^{-1}; Table 2). These margin sediments are about 80% marine biogenic material [51], further reducing the contribution that continental detritus could make to the ^{10}Be content of sediments at these sites. The sites of V19-28 and V19-29 are located seaward of the Peru-Chile trench, which would tend to trap detrital material moving seaward from the continent. No large rivers occur in nearby regions of South America which could introduce significant amounts of dissolved ^{10}Be. While leaching of aerosol dust can be an important local source of Al and ^{9}Be in surface ocean waters, this seems not to be the case for ^{10}Be [25]. Ruling out these potential local sources for the excess ^{10}Be in the sediments from V19-28 and V19-29 leads us to conclude that the higher ^{10}Be/^{230}Th ratios there

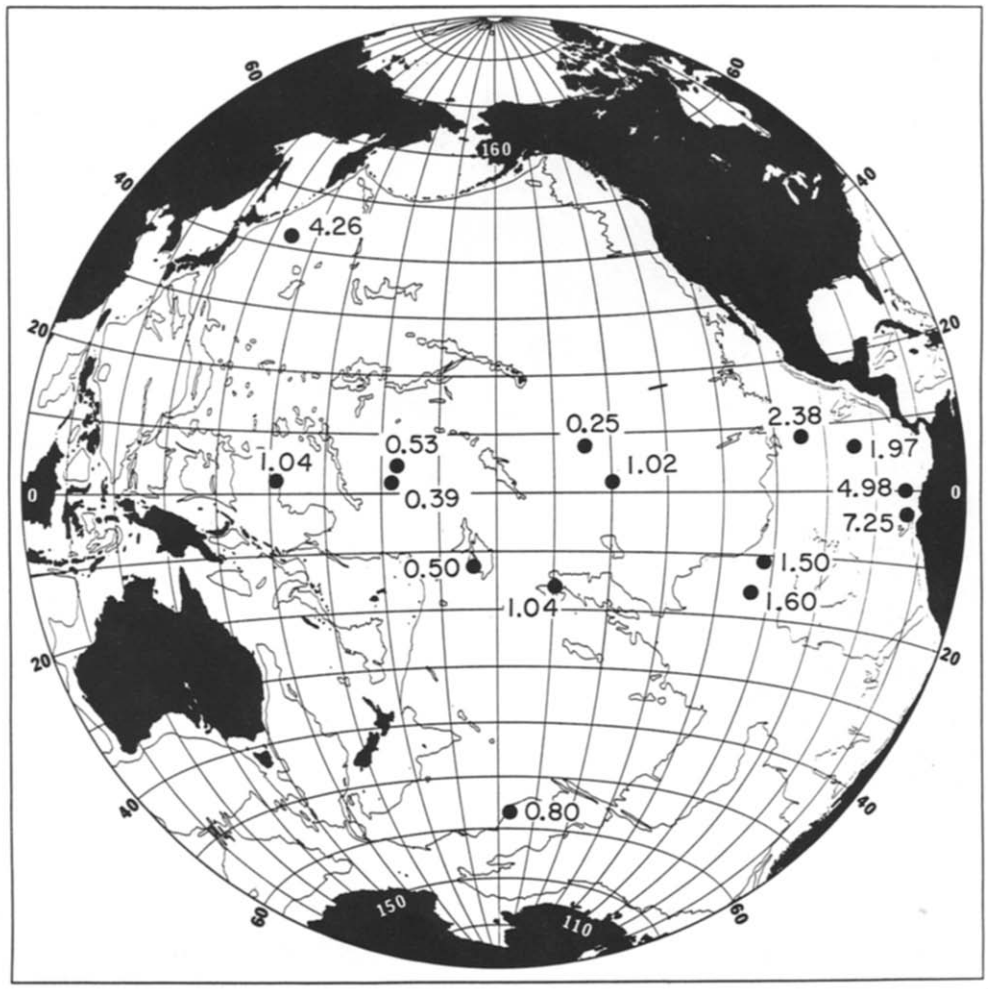

Fig. 2. Deposition Index values for ^{10}Be from Tables 3 and 4. I_D[Be] values are proportional to the scavenging rate of ^{10}Be at each site with a value of 1.0 approximately representing the ocean-wide average ^{10}Be scavenging rate.

must reflect preferential removal of ^{10}Be from seawater at ocean margins.

4.4. Deposition rates and residence times of ^{10}Be in the Pacific

Normalizing ^{10}Be concentrations to ^{230}Th allowed us to establish unequivocally that ^{10}Be is preferentially removed from the ocean at margins. Normalizing to ^{230}Th will also permit us to quantify rates of ^{10}Be removal in different ocean regions and, from that, to evaluate residence times of ^{10}Be with respect to chemical scavenging for each region.

Taking the average deposition rate of ^{230}Th to be everywhere equivalent to its rate of production in the overlying water column, the known rate of ^{230}Th production in seawater (P_{Th}; dpm cm^{-2} ka^{-1}) can be used to quantify regional average ^{10}Be deposition rates (S_{Be}; at cm^{-2} ka^{-1}) [21–23] as:

$$S_{Be} = P_{Th} \cdot \left(^{10}\mathrm{Be}/\mathrm{xs}^{230}\mathrm{Th}\right)_0 \quad (5)$$

^{230}Th is produced at a rate of $0.0026Z$ dpm cm^{-2} ka^{-1} where Z is the water depth in meters. ^{10}Be deposition rates calculated from equation (5) are presented in Table 5. These results show that the deposition rate of ^{10}Be approximately equals its global average rate of production (1.21×10^6 at cm^{-2} a^{-1} [45]) in open-ocean sediments containing appreciable amounts of $CaCO_3$ where accumu-

TABLE 5

Deposition rates and residence times of ^{10}Be in the Pacific Ocean

Sample site [a]	Water depth (m)	^{230}Th production rate (dpm cm^{-2} ka^{-1})	^{10}Be/xs^{230}Th [b] (10^9 at dpm^{-1})	^{10}Be deposition rate [c] (10^6 at cm^{-2} a^{-1})	^{10}Be residence time [d] (years)
V18-299	4284	11.14	0.127	1.41	515
RC11-210	4420	11.49	0.125	1.44	523
V28-238	3120	8.11	0.127	1.03	515
TT154-10	3225	8.39	0.183	1.53	357
V19-55	3177	8.26	0.195	1.61	335
V19-28	2720	7.07	0.607	4.29	108
V19-29	3157	8.21	0.884	7.26	74
V28-258	5528	14.37	0.061 [e]	0.88	1072
			0.021 [f]	0.30	3114
MSN 147G	5110	13.29	0.031	0.41	2109
NOVA III-13	5351	13.91	0.065	0.90	1006
NOVA III-16	5585	14.52	0.048	0.70	1362
MSN 96	4760	12.38	0.098	1.21	667
DSDP 580	5385	14.00	0.52	7.28	126
MANOP H	3600	9.36	0.24 [g]	2.25	272
MANOP M	3100	8.03	0.29 [g]	2.34	225

[a] Locations of the first 7 cores are given in Table 1 and the others in Table 4.
[b] Decay corrected to time of deposition.
[c] Calculated according to equation (5) in text.
[d] Calculated according to equation (6) in text.
[e] Measured ratio in core-top sediments.
[f] Ratio obtained by extrapolating profiles to zero depth (see text).
[g] Ratios represent average values for sediment trap samples collected at water depths > 2000 m.

lation rates are ~ 1 cm ka^{-1} (our open-ocean sites in Table 1). ^{10}Be consistently accumulates at rates much less than its global production rate in deeper abyssal red-clay regions (first 5 sites in Table 4). In ocean-margin regions, on the other hand, ^{10}Be is scavenged from the water column at rates as much as six times its average rate of production in the atmosphere, the excess ^{10}Be being supplied to the margins by lateral mixing from the open ocean. If the average ^{10}Be deposition rate (6.28×10^6 at cm^{-2} a^{-1}) at the three margin sites (V19-28, V19-29 and DSDP 580) is typical of all ocean margin regions, if such regions constitute 10% of the area of the Pacific Ocean, and if 1.21×10^6 at cm^{-2} a^{-1} is an appropriate value for the average rate of ^{10}Be supply to the Pacific, then about 50% of the ^{10}Be introduced into the ocean is removed at the margins. As the ^{10}Be deposition rate at margins is based on results from only three sites, there is a large uncertainty in this estimate. Future studies will reduce this uncertainty, but they should not change the basic conclusion that a large proportion of the ^{10}Be supplied to the Pacific Ocean is deposited in margin sediments.

For each site, the residence time of ^{10}Be with respect to chemical scavenging from the water column can be calculated from the inventory of ^{10}Be in the water column, I_{Be}, and the ^{10}Be deposition rate, S_{Be}, as:

$$\tau_{Be} = I_{Be}/S_{Be} \quad (6)$$

^{10}Be inventories are calculated for each site using the average ^{10}Be concentration of Pacific seawater of 1700 at g^{-1} [24]. Values of τ_{Be} range from > 1000 years in the red clay regions through ~ 500 years at our three "open-ocean" sites to a value of only ~ 100 years for the margin sites (Table 5). There are too few data at this time to estimate the Pacific-wide average residence time of Be, but a value of ~ 500 years would be obtained for a 3800 m deep ocean with an average I_D[Be] of 1.0. More important than the ocean-wide average value of τ_{Be} is the striking difference between ^{10}Be deposition rates and residence times in deep

open-ocean waters and the those in ocean-margin regions. The much greater scavenging rate at margins, coupled with lateral mixing, leads to much higher rates of ^{10}Be deposition in ocean-margin sediments (see section 4.8).

4.5. Uncertainties associated with boundary scavenging of ^{230}Th

Because the deposition rates and residence times discussed in the preceding section were obtained by normalizing measured ^{10}Be concentrations in sediments to a tracer with a known production rate (^{230}Th), they are free from biases caused by local sediment transport. However, this approach is not totally free from uncertainty because boundary scavenging of ^{230}Th is assumed to be negligible; i.e., ^{230}Th is assumed to be scavenged from the water column in the region in which it is produced. Particulate ^{230}Th fluxes measured with sediment traps and model calculations suggest that as much as 20% of the ^{230}Th produced in the open ocean may be transported to margins prior to burial [5,6,12,13]. Uncertainty in the extent of lateral redistribution of ^{230}Th limits the precision with which we can assign scavenging rates of ^{10}Be. Some constraints can be placed on ^{10}Be fluxes, however, because we know that the tendency for redistribution is from the open ocean to margins. Consequently, open-ocean ^{10}Be fluxes estimated by this approach represent upper limits, whereas calculated ^{10}Be fluxes at ocean margins represent lower limits. Regional values of τ_{Be} are similarly affected, so 1000 years is a lower limit for open-ocean regions while 100 years is an upper limit for the margin sites. If there is an error in our approach, then it is in the direction that boundary scavenging of ^{10}Be is even more extensive than we have estimated.

Our approach of normalizing ^{10}Be concentrations to ^{230}Th has another distinct advantage in that it allows the deposition rate of ^{10}Be at any site to be estimated by analyzing a single sample for ^{10}Be and ^{230}Th. With this approach, it will be feasible to survey entire ocean basins to more completely assess the nature of ^{10}Be removal from the oceans.

4.6. Independent estimates of ^{10}Be accumulation rates

^{10}Be deposition rates can be calculated independently using sediment mass accumulation rate (MAR) data where available to test our results and interpretation derived by normalizing ^{10}Be concentrations to ^{230}Th. At the margin location of V19-28, we have used nuclide activities (Table 3) and MAR [51] from the upper Holocene record (17–19 cm) to calculate accumulation rates of ^{10}Be (10.1×10^6 at cm^{-2} a^{-1}) and ^{230}Th (16.7 dpm cm^{-2} ka^{-1}). The accumulation rate of ^{10}Be is 8.3 times its global average production rate whereas unsupported ^{230}Th is accumulating at a rate equivalent to 2.36 times its rate of production in the overlying water column. The factor of 2.36 seems too high to reflect boundary scavenging of ^{230}Th, so it may indicate that local sediment transport has focussed sediment to the core site. However, the factor of 2.36 represents an upper limit for sediment focussing, from which a lower limit for the rate of ^{10}Be removal from the water column in this region can be set at 4.3×10^6 at cm^{-2} a^{-1} (10.1/2.36). Scavenging of ^{10}Be to these margin sediments occurs at a rate no less than 3.5 times greater than its average global rate of production (1.21×10^6 at cm^{-2} a^{-1}).

Eisenhauer et al. [47] reported a long-term average ^{10}Be accumulation rate of 11.5×10^6 at cm^{-2} a^{-1} at the site of DSDP-580 in a margin region site off Japan where Yang et al. [7] documented intense boundary scavenging of ^{231}Pa. Brown et al. [20] measured ^{10}Be concentrations in surface sediments off southern California and used average sediment mass accumulation rates to estimate ^{10}Be deposition rates of about 10×10^6 at cm^{-2} a^{-1} for that ocean-margin region. These results consistently indicate rates of ^{10}Be deposition in margin sediments much greater than its global average rate of supply.

The MAR for the depth interval of RC11-210 from which our samples were taken was 0.89 g cm^{-2} ka^{-1} [52]. Multiplying this MAR by our measured ^{10}Be content gives a ^{10}Be deposition rate of 2.65×10^6 at cm^{-2} a^{-1}, about twice our estimated average rate of ^{10}Be scavenging from equatorial Pacific waters (Table 5). Similarly, using the initial unsupported ^{230}Th activity of 23.85 dpm g^{-1} (Table 3), a ^{230}Th accumulation rate of 21.2 dpm cm^{-2} ka^{-1} is obtained, nearly twice the rate of ^{230}Th production in the overlying 4420 m water column (11.5 dpm cm^{-2} ka^{-1}). The extent to which accumulation of ^{10}Be and ^{230}Th exceed their respective production rates could reflect

lateral transport of dissolved nuclides to a region of enhanced scavenging under the equatorial zone of high productivity. It could also reflect local focussing of sediments to the position where the core was collected, or, it could result from an error in assigning a chronology to the upper portion of the core (M. Lyle, personal communication). At this time there is no way to choose the correct explanation from among these possibilities. This example illustrates the value of normalizing the accumulation rates of elements, nuclides, or solid phases to a tracer such as ^{230}Th whose known source permits lateral redistribution to be identified and regional burial rates to be evaluated.

Along with their ^{10}Be results, Amin et al. [46] reported sediment accumulation rates based on ^{230}Th/^{232}Th profiles and in situ sediment densities from which accumulation rates of ^{10}Be can be calculated. These are 0.42, 0.12, 0.47 and 0.81 $\times$ 10^6 at cm^{-2} a^{-1} for MSN 147G, NOVA III-13, NOVA III-16 and MSN 96 respectively. Where inconsistencies exist between these ^{10}Be accumulation rates and those obtained by normalizing to ^{230}Th (Table 5), the former tend to be lower. This could indicate a net lateral export of ^{230}Th from these regions, but the inconsistency is not systematic, as would be the case if ^{230}Th export were the cause. This suggests that errors may also exist for the estimated sediment accumulation rates or the sediment densities. In any case, the deposition rate of ^{10}Be in pelagic red clays is much less than its global average production rate, whereas ^{10}Be is deposited in ocean-margin sediments at rates greatly exceeding its global average production rate.

4.7. Boundary scavenging of ^{10}Be in the Atlantic Ocean

By combining results from various sources, we can show that boundary scavenging must also influence the removal of ^{10}Be from the North Atlantic Ocean. ^{10}Be and ^{230}Th data are available from two open-ocean sites. Somayajulu et al. [53] studied a core collected at 32°N on the Mid-Atlantic Ridge. A Holocene ^{10}Be/xs^{230}Th$_0$ ratio of 0.032 $\times$ 10^9 (at dpm^{-1}) can be calculated from their results. At another open-ocean site (40°36′N, 21°42′W; 3485 m), Southon et al. [54] reported a Holocene ^{10}Be/xs^{230}Th$_0$ ratio of 0.070 $\times$ 10^9. Results are also available for two ocean-margin sites. Holocene sediments off northwest Africa contain a ^{10}Be/xs^{230}Th$_0$ ratio of 0.15 $\times$ 10^9 (compare Th results from [55] with Be results from [19] for core 12310: 23°30′N, 18°43′W; 3080 m). We have analyzed surficial sediments from two cores collected on the continental slope south of New England (OCE-152 BC5: 38°09′N, 70°56′W; 2691 m; OCE-152 BC9: 39°42′N, 70°55′W; 1981 m) where we obtained an average ^{10}Be/xs^{230}Th$_0$ ratio of 0.40 $\times$ 10^9. The ^{10}Be/xs^{230}Th$_0$ ratio in margin sediments is as much as an order of magnitude greater than in open-ocean sediments, indicating that preferential removal of ^{10}Be at ocean margins also occurs in the North Atlantic.

4.8. Conditions responsible for boundary scavenging

Here the basic principles of boundary scavenging are reviewed to illustrate how certain particle-reactive elements (Be or Pa) can follow distinctly different pathways of removal from the ocean compared to other particle-reactive elements such as ^{230}Th. Bacon [12] reviewed boundary scavenging and provided a quantitative discussion of the processes that lead to the separation of ^{231}Pa and ^{230}Th between their production in, and removal from, the ocean. A more general illustration is given here of the conditions and processes which lead to boundary scavenging. Important parameters for this illustration include: the reactivity of each element toward scavenging by particles (often expressed as a residence time with respect to scavenging), the magnitude of the particle flux in each region, and the lateral mixing rate in the ocean. For simplicity, it is first assumed that particles have a homogeneous composition throughout the ocean so that differential scavenging reflects only the relative particle flux at each location, and not the surface chemical properties of the particles themselves. The influence of particle composition is discussed below.

Imagine a two-dimensional ocean where each wall represents a margin or boundary. Production of each tracer is uniform throughout the ocean (Fig. 3A). A minimum time scale required for lateral mixing to significantly redistribute a tracer from the center of the basin to the margin, T, is approximately equal to X^2/K_H, where X is the scale length (half width) of the basin and K_H is

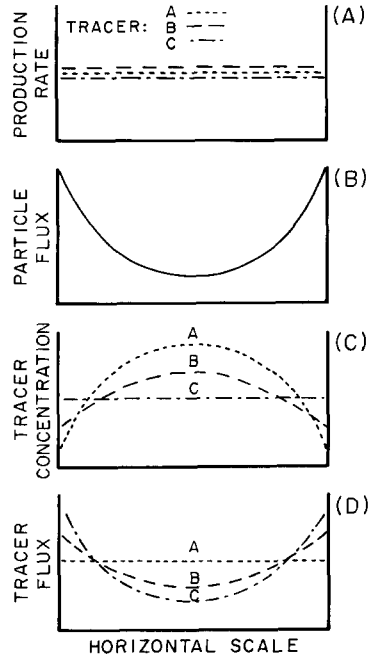

Fig. 3. This series of panels illustrates how lateral mixing rate and differential particle flux influence boundary scavenging of three tracers having different reactivities toward chemical scavenging. Fluxes, concentrations, and production rates are expressed in arbitrary relative units. The purpose of this figure is to help clarify the boundary scavenging concept, not to rigorously express any quantitative relationships. A. Production rates of the three tracers are uniform across an ocean basin. B. Particle fluxes are higher at ocean margins than in the interior. C. The concentration of each tracer dissolved in the water column is established by the relationship between the scavenging rate of the tracer ($A \gg B \gg C$) and the lateral mixing rate of the ocean. D. The flux of each tracer is proportional to the product of the tracer concentration times the particle flux. See text for details.

the horizontal mixing coefficient. A typical ocean basin might have $X = 3000$ km and $K_H = 3 \times 10^7$ cm^2 s^{-1} [56], in which case $T = 95$ years. Like the real ocean, the flux of particles is high at the margins and low in the interior (Fig. 3B). Because a homogeneous particle composition is assumed, the rate constant for scavenging of a tracer at any particular site is simply proportional to the particle flux. Reactivity of the tracers increases in the order $C < B < A$ and residence times of the tracers in the ocean interior are set to be: $\tau_A = 0.1T$, $\tau_B = 1.0T$, and $\tau_C = 10T$. The relative concentration of each tracer along a transect across the ocean is shown in Fig. 3C, and the relative downward particulate flux of each tracer is presented in Fig. 3D.

In this illustration, throughout the ocean the flux of tracer A approximately equals its rate of production in the water column because its residence time is too short for lateral mixing to transport significant quantities from interior regions to the margins. The residence time of tracer C, on the other hand, is sufficiently long ($10T$) that lateral mixing nearly homogenizes its concentration throughout the basin. Therefore, the flux of tracer C is almost directly proportional to the particle flux. Tracer B, for which $\tau = T$, has an intermediate behavior. Significant lateral transport to margins occurs, but the concentration of B is not uniform throughout the ocean. Consequently, the flux of B is neither uniformly equivalent to its production rate nor is it directly proportional to the flux of particulate matter.

While this simple illustration is primarily intended to help clarify the boundary scavenging concept, the similarity between ^{230}Th, ^{231}Pa and ^{10}Be and the tracers A, B and C respectively is not entirely unintentional. As pointed out by Bacon [12], the relative time scales of lateral mixing and of chemical scavenging of an element is an important factor governing the extent to which boundary scavenging influences the removal of the element from the ocean. Boundary scavenging exerts a greater influence over elements for which $\tau > T$ than for elements with $\tau < T$.

Particle composition also influences scavenging intensity. Manganese oxide coatings on particles [1,6], biogenic opal [15], and clays [54] have been implicated as phases having a pronounced influence over the scavenging of ^{231}Pa and ^{10}Be. Although boundary scavenging enhances the deposition of both ^{10}Be and ^{231}Pa at margins compared to central ocean gyres, the influence of particle composition on the scavenging of ^{231}Pa and ^{10}Be seems to be different. For example, whereas metalliferous sediments on the EPR (TT154-10, V19-55) have ^{231}Pa/^{230}Th ratios approaching those of the margin sediments (Table 3), the ^{10}Be/^{230}Th ratio of the metalliferous sediments is only about 50% greater than the ratio in our other "open-ocean" sites listed in Table 1. Our results for metalliferous sediments are consistent with laboratory studies [57] showing that the partition coefficient (K_D) for adsorption of Be

TABLE 6

^{10}Be/xs^{230}Th ratios in manganese nodules

Nodule	Latitude	Longitude	Water depth (m)	^{10}Be/xs^{230}Th [a] (10^9 at dpm^{-1})	Reference
A47-16-4	09°02'N	151°11'W	5040	0.033	[69]
TF-5	13°53'S	150°35'W	3623	0.050	[69]
R/V Vitiaz	26°48'S	108°15'E	5258	0.025	[69]
SCHW-1D	30°N	140°W	3480	0.011	[70]
TDK 44	12°49'N	118°52'E	1900	0.035	[71]
TDK 40	12°21'N	118°49'E	1000	0.188	[71]

[a] Decay-corrected to time of deposition by extrapolating profiles to nodule surface.

onto marine particles does not depend on the MnO_2 content of the particles and with field studies [6] showing a strong dependence of K_D for Pa on the Mn content of marine particles. This is also consistent with published results for manganese nodules. Whereas Mn nodules preferentially incorporate Pa relative to Th [58], the ^{10}Be/^{230}Th ratio at the surface of Mn nodules (Table 6) tends to be less than or equal to the average value for deep-sea sediments. The one exception (TDK 40) is a shallow water nodule from an ocean-margin region. While particle composition may influence the nature and intensity of boundary scavenging, metal oxide coatings probably contribute little, if at all, to the boundary scavenging of ^{10}Be. Whether scavenging of ^{10}Be is predominantly controlled by the flux of clays, as suggested by Southon et al. [54], or by some other factor, remains to be determined.

5. Conclusions

Enhanced scavenging at ocean margins leads to a preferential deposition of ^{10}Be in ocean-margin sediments. ^{10}Be is scavenged from seawater and deposited in ocean-margin sediments at rates at least an order of magnitude greater than in the open ocean. ^{10}Be shows an even greater enhancement of deposition at margins than occurs for ^{231}Pa. However, the processes responsible for boundary scavenging of ^{10}Be and ^{231}Pa may be different. Whereas metalliferous oxyhydroxides strongly enhance the scavenging of Pa, they have only a small effect on Be.

Because the rate of ^{10}Be deposition in marine sediments varies significantly from one region to another, it is impossible to define an ocean-wide average rate of ^{10}Be supply by measuring ^{10}Be accumulation rates in a few cores. An average flux of ^{10}Be to the ocean can only be obtained by first examining a number of sites representative of different major oceanic environments, and then by normalizing ^{10}Be contents of the sediments at those sites to a tracer with a known source, such as ^{230}Th, to eliminate biases due to physical transport of sediments. ^{10}Be deposition rates in the Pacific Ocean range from 0.4 to 7.3×10^6 at cm^{-2} a^{-1} among the sites examined here. Using these deposition rates and an average concentration of ^{10}Be in Pacific Ocean water to estimate inventories, we calculate regional residence times for ^{10}Be in the Pacific ranging from ~ 100 years at ocean margins to > 1000 years in deep open-ocean regions.

Production of ^{10}Be is proportional to the cosmic ray flux, as modulated by solar activity and the Earth's magnetic field. There has been widespread interest in trying to use ^{10}Be deposition records to obtain an indirect measure of how one or more of these parameters (cosmic ray flux, magnetic field strength, solar activity) have changed with time. Several investigators have examined marine sediment records for evidence of temporal variability in the rate of ^{10}Be accumulation, from which variability in the rate of ^{10}Be production could be inferred [53,54,59–66]. With as much as 50% of the ^{10}Be supplied to the oceans being removed at margins, a major change in the nature of boundary scavenging could lead to a significant redistribution of ^{10}Be burial within the ocean. A change in a local rate of ^{10}Be deposition in marine sediments could reflect such a redistribution rather than a change in the global rate of ^{10}Be production. Consequently, temporal variability in the rate of

^{10}Be production can never be evaluated unambiguously from the ^{10}Be deposition record in a single core, or even from the records of a few cores. Before temporal variability in the global rate of ^{10}Be production can be assessed from marine sediment records, we will need a better understanding of the processes that lead to the preferential removal of ^{10}Be at ocean margins and of how these processes have changed with time.

Acknowledgements

A. Mangini and G. Raisbeck provided advice which helped us develop our method for ^{10}Be analysis. R. Fairbanks and J. Wright produced the ^{18}O and ^{13}C results which provided the chronology for V18-299. B. Hamelin helped obtain the ^{230}Th/^{232}Th ratios by mass spectrometry. Discussions with M. Bacon over the years have advanced our ideas about boundary scavenging, and he, along with M. Monaghan and C. Measures, provided useful comments on earlier drafts of this manuscript. Various portions of this work were supported by the Department of Energy through Award No. DE-FG02-87-ER60555 AA, NASA (NCC 5-29C), NSF (ATM 88-13056; OCE89-11427) and by a start-up grant from LDGO. Lamont-Doherty Geological Observatory of Columbia University Contribution No. 4536.

References

1 D.W. Spencer, M.P. Bacon and P.G. Brewer, Models of the distribution of ^{210}Pb in a section across the North Equatorial Atlantic Ocean, J. Mar. Res. 39, 119–138, 1981.
2 M.P. Bacon, D.W. Spencer and P.G. Brewer, ^{210}Pb/^{226}Ra and ^{210}Po/^{210}Pb disequilibria in seawater and suspended particulate matter, Earth Planet. Sci. Lett. 32, 277–296, 1976.
3 R. Carpenter, J.T. Bennett and M.L. Peterson, ^{210}Pb activities in and fluxes to the sediments of the Washington continental slope and shelf, Geochim. Cosmochim. Acta 45, 1155–1172, 1981.
4 J.K. Cochran, M.P. Bacon, S. Krishnaswami and K.K. Turekian, ^{210}Pb and ^{210}Po distributions in the central and eastern Indian Ocean, Earth Planet. Sci. Lett. 65, 433–452, 1983.
5 R.F. Anderson, M.P. Bacon and P.G. Brewer, Removal of ^{203}Th and ^{231}Pa from the open ocean, Earth Planet. Sci. Lett. 62, 7–23, 1983.
6 R.F. Anderson, M.P. Bacon and P.G. Brewer, Removal of ^{230}Th and ^{231}Pa at ocean margins, Earth Planet. Sci. Lett. 66, 73–90, 1983.
7 H.-S. Yang, Y. Nozaki, Y. Sakai and A. Masuda, The distribution of ^{230}Th and ^{231}Pa in the deep surface sediments of the Pacific Ocean, Geochim. Cosmochim. Acta 50, 81–89, 1986.
8 G.B. Shimmield, J.W. Murray, J. Thomson, M.P. Bacon, R.F. Anderson and N.B. Price, The distribution and behavior of ^{230}Th and ^{231}Pa at an ocean margin, Baja California, Mexico, Geochim. Cosmochim. Acta 50, 2499–2507, 1986.
9 M. Koide and E.D. Goldberg, Transuranic nuclides in two coastal marine sediments off Peru, Earth Planet. Sci. Lett. 57, 263–277, 1982.
10 M. Koide, J.J. Griffin and E.D. Goldberg, Records of plutonium fallout in marine and terrestrial samples, J. Geophys. Res. 80, 4153–4162, 1975.
11 M. Koide, E.D. Goldberg and V.F. Hodge, ^{241}Pu and ^{241}Am in sediments from coastal basins off California and Mexico, Earth Planet. Sci. Lett. 48, 250–256, 1980.
12 M.P. Bacon, Tracers of chemical scavenging in the ocean: boundary effects and largescale chemical fractionation, Philos. Trans. R. Soc. London, Ser. A 325, 147–160, 1988.
13 M.P. Bacon, C.-A. Huh, A.P. Fleer and W.G. Deuser, Seasonality in the flux of natural radionuclides and plutonium in the deep Sargasso Sea, Deep-Sea Res. 32, 273–286, 1985.
14 D. Kadko, ^{230}Th, ^{226}Ra and ^{222}Rn in abyssal sediments, Earth Planet. Sci. Lett. 49, 360–380, 1980.
15 K. Taguchi, K. Harada and S. Tsunogai, Particulate removal of ^{230}Th and ^{231}Pa in the biologically productive northern North Pacific, Earth Planet. Sci. Lett. 93, 223–232, 1989.
16 L. Brown, Applications of accelerator mass spectrometry, Annu. Rev. Earth Planet. Sci. 12, 39–59, 1984.
17 G.M. Raisbeck and F. Yiou, Production of long-lived cosmogenic radionuclides and their applications, Nucl. Instrum. Methods B5, 91–99, 1984.
18 L. Brown, ^{10}Be: recent applications in Earth sciences, Philos. Trans. R. Soc. London, Ser. A 323, 75–86, 1987.
19 A. Mangini, M. Segl, G. Bonani, H.J. Hofmann, E. Morenzoni, M. Nessi, M. Suter, W. Wolfli and K.K. Turekian, Mass Spectrometric ^{10}Be dating of deep-sea sediments applying the Zurich tandem accelerator, Nucl. Instrum. Methods B5, 353–358, 1984.
20 L. Brown, J. Klein and R. Middleton, Anomalous isotopic concentrations in the sea off Southern California, Geochim. Cosmochim. Acta 49, 153–157, 1985.
21 M.P. Bacon and J.N. Rosholt, Accumulation of ^{230}Th, ^{231}Pa, and some transition metals on the Bermuda Rise, Geochim. Cosmochim. Acta 46, 651–666, 1982.
22 M.P. Bacon, Glacial to interglacial changes in carbonate and clay sedimentation in the Atlantic Ocean estimated from ^{230}Th measurements, Isot. Geosci. 2, 97–111, 1984.
23 D.O. Suman and M.P. Bacon, Variations in Holocene sedimentation in the North American Basin determined from Th-230 measurements, Deep-Sea Res. 36, 869–878, 1989.
24 M. Kusakabe, T.-L. Ku, J.R. Southon, J.S. Vogul, D.E. Nelson, C.I. Measures and Y. Nozaki, Distribution of ^{10}Be and ^{9}Be in the Pacific Ocean, Earth Planet. Sci. Lett. 82, 231–240, 1987.
25 T.-L. Ku, M. Kusakabe, C.I. Measures, J.R. Southon, J.S. Vogul, D.E. Nelson and S. Nakaya, Be isotope distribution

in the western North Atlantic: a comparison to the Pacific. Deep-Sea Res., submitted.
26 P.R. Betzer, W.J. Showers, E.A. Laws, C.D. Winn, G.R. DiTullio and P.M. Kroopnick, Primary productivity and particle fluxes on a transect of the equator at 153° W in the Pacific Ocean, Deep-Sea Res. 31, 1–11, 1984.
27 J. Dymond and R. Collier, Biogenic particle fluxes in the equatorial Pacific: evidence for both high and low productivity during the 1982–1983 El Niño, Global Biogeochem. Cycles 2, 129–137, 1988.
28 S. Honjo, S.J. Manganini and J.J. Cole, Sedimentation of biogenic matter in the deep ocean, Deep-Sea Res. 29, 609–625, 1982.
29 M. Bender, W. Broecker, V. Gornitz, U. Middel, R. Kay, S.-S. Sun and P. Biscaye, Geochemistry of three cores from the East Pacific Rise, Earth Planet. Sci. Lett. 12, 425–433, 1971.
30 G.B. Shimmield and N.B. Price, The scavenging of U, ^{230}Th and ^{231}Pa during pulsed hydrothermal activity at 20° S, East Pacific Rise, Geochim. Cosmochim. Acta 52, 669–677, 1988.
31 R.F. Anderson and A.P. Fleer, Determination of natural actinides and plutonium in marine particulate material, Anal. Chem. 54, 1142–1147, 1982.
32 M. Suter, R. Balzer, G. Bonani, H.J. Hofmann, E. Morenzoni, M. Nessi, W. Wolfli, M. Andree, J. Beer and H. Oeschger, Precision measurement of ^{14}C in AMS—some results and prospects, Nucl. Instrum. Methods B5, 117–122, 1984.
33 S.R. Taylor, Abundance of chemical elements in the continental crust: a new table, Geochim. Cosmochim. Acta 28, 1273–1286, 1964.
34 J.H. Chen, G.J. Wasserburg, K.L. von Damm and J.M. Edmond, The U-Th-Pb systematics in hot springs on the East Pacific Rise at 21° N and Guaymas Basin, Geochim. Cosmochim. Acta 50, 2467–2479, 1986.
35 J.H. Chen, U. Th, and Pb Isotopes in hot springs on the Juan de Fuca Ridge, J. Geophys. Res. 92, 11411–11415, 1987.
36 W.S. Moore, The thorium isotope content of ocean water, Earth Planet. Sci. Lett. 53, 419–426, 1981.
37 Y. Nozaki, Y. Horibe and H. Tsubota, The water column distributions of thorium isotopes in the western North Pacific, Earth Planet. Sci. Lett. 54, 203–216, 1981.
38 Y. Nozaki and Y. Horibe, Alpha-emitting thorium isotopes in northwest Pacific deep waters, Earth Planet. Sci. Lett. 65, 39–50, 1983.
39 Y. Nozaki, H.S. Yang and M. Yamada, Scavenging of thorium in the ocean, J. Geophys. Res. 92, 772–778, 1987.
40 C.-A. Huh and T.M. Beasley, Profiles of dissolved and particulate thorium isotopes in the water column of coastal Southern California, Earth Planet. Sci. Lett. 85, 1–10, 1987.
41 D.K. Rea, M. Leinen and T.R. Janecek, Geologic approach to the long-term history of atmospheric circulation, Science 227, 721–725, 1985.
42 D.K. Rea, B.C. Chambers and B.G. Dempsey, Eolian dust input to the North Pacific Ocean during the past 30,000 years, EOS 64, 739, 1983.
43 T.R. Janacek and D.K. Rea, Quaternary fluctuations in the Northern Hemisphere Trade Winds and Westerlies, Quat. Res. 24, 150–163, 1985.
44 K.W. Bruland and K.H. Coale, Surface water ^{234}Th/^{238}U disequilibria: spatial and temporal variations of scavenging rates within the Pacific Ocean, in: Dynamic Processes in the Chemistry of the Upper Ocean, J.D. Burton, P.G. Brewer and R. Chesselet, eds., pp. 159–172, Plenum, New York, N.Y., 1986.
45 M.C. Monaghan, S. Krishnaswami and K.K. Turekian, The global average production rate of ^{10}Be, Earth Planet. Sci. Lett. 76, 279–287, 1986.
46 B.S. Amin, D. Lal and B.L.K. Somayajulu, Chronology of marine sediments using the ^{10}Be method: Intercomparison with others, Geochim. Cosmochim. Acta 39, 1187–1192, 1975.
47 A. Eisenhauer, A. Mangini, M. Segl, J. Beer, G. Bonani, M. Suter and W. Wolfli, High resolution ^{10}Be and ^{230}Th profiles in DSDP Site 580, Nucl. Instrum. Methods Phys. Res. B29, 326–331, 1987.
48 P. Sharma, R. Mahannah, W.S. Moore, T.L. Ku and J.R. Southon, Transport of ^{10}Be and ^{9}Be in the ocean, Earth Planet. Sci. Lett. 86, 69–76, 1987.
49 R.N. Mahannah, Jr., Uranium and thorium series isotopes in sediment trap material from MANOP Sites H and M in the eastern Pacific Ocean, 78 pp., M.S. Thesis, University of South Carolina, 1984.
50 L. Brown, M.J. Pavich, R.E. Hickman, J. Klein and R. Middleton, Erosion of the eastern United States observed with ^{10}Be, Earth Surface Processes and Landforms 13, 441–457, 1988.
51 M. Lyle, D.W. Murray, B.P. Finney, J. Dymond, J.M. Robbins and K. Brooksforce, The record of late Pleistocene biogenic sedimentation in the eastern tropical Pacific Ocean, Paleoceanography 3, 39–59, 1988.
52 J.M. Chuey, D.K. Rea and N.G. Pisias, Late Pleistocene paleoclimatology of the central North Pacific: A quantitative record of eolian and carbonate deposition, Quat. Res. 28, 323–339, 1987.
53 B.L.K. Somayajulu, P. Sharma and W.H. Berger, ^{10}Be, ^{14}C and U-Th decay series nuclides and δ^{18}O in a box core from the central North Atlantic, Mar. Geol. 54, 169–180, 1983.
54 J.R. Southon, T.-L. Ku, D.E. Nelson, J.L. Reyss, J.C. Duplessy and J.S. Vogel, ^{10}Be in a deep-sea core: implications regarding ^{10}Be production changes over the past 420 ka, Earth Planet. Sci. Lett. 85, 356–364, 1987.
55 A. Mangini and L. Diester-Haass, Excess Th-230 in sediments off NW Africa traces upwelling in the past, in: Coastal Upwelling: Its Sedimentary Record, E. Suess and J. Thiede, eds., pp. 455–470, Plenum, New York, N.Y., 1983.
56 J.L. Sarmiento, C.G.H. Rooth and W.S. Broecker, Radium-228 as a tracer of basin wide processes in the abyssal ocean. J. Geophys. Res. 87, 9694–9698, 1982.
57 L.S. Balistrieri and J.W. Murray, The surface chemistry of sediments from the Panama Basin: The influence of Mn oxides on metal adsorption, Geochim. Cosmochim. Acta 50, 2235–2243, 1986.
58 T.L. Ku and W.S. Broecker, Radiochemical studies on manganese nodules of deep-sea origin, Deep-Sea Res. 16, 625–637, 1969.
59 B.L.K. Somayajulu, Analysis of causes for the beryllium-10 variations in deep sea sediments, Geochim. Cosmochim. Acta 41, 909–913, 1977.

60 S. Tanaka, T. Inoue and M. Imamura, The ^{10}Be method of dating marine sediments—comparison with the paleomagnetic method, Earth Planet. Sci. Lett. 37, 55–60, 1977.
61 T. Inoue and S. Tanaka, ^{10}Be in marine sediments, Earth's environment and cosmic rays, Nature 277, 209–210, 1979.
62 S. Tanaka and T. Inoue, ^{10}Be dating of North Pacific sediment cores up to 2.5 million years B.P., Earth Planet. Sci. Lett. 45, 181–187, 1979.
63 S. Tanaka and T. Inoue, ^{10}Be evidence for geochemical events in the North Pacific during the Pliocene, Earth Planet. Sci. Lett. 49, 34–38, 1980.
64 P. Sharma, S.K. Bhattacharya and B.L.K. Somayajulu, Beryllium-10 in deep sea sediments and cosmic ray intensity variations, 18th Int. Cosmic Ray Conf., Bangalore, India, OG Sessions 2, 337–340, 1983.
65 P. Sharma and B.L.K. Somayajulu, Implications of precise ^{10}Be measurements in deep-sea sediments, Isot. Geosci. 2, 89–96, 1984.
66 G.M. Raisbeck, F. Yiou, D. Bourles and D.V. Kent, Evidence for an increase in cosmogenic ^{10}Be during a geomagnetic reversal, Nature 315, 315–317, 1985.
67 W. Broecker, M. Klas, N. Regano-Bevan, G. Mathieu, A. Mix, M. Andree, H. Oeschger, W. Wolfli, M. Suter, G. Bonani, H.J. Hofmann, M. Nessi and E. Morenzoni, Accelerator mass spectrometry radiocarbon measurements on marine carbonate samples from deep sea cores and sediment traps, Radiocarbon 30, 261–295, 1988.
68 T.C. Moore Jr., L.H. Burckle, K. Geitzenauer, B. Luz, A. Molina-Cruz, J.H. Robertson, H. Sachs, C. Sancetta, J. Thiede, P. Thompson and C. Wenkam, The reconstruction of sea surface temperatures in the Pacific Ocean of 18,000 B.P., Mar. Micropaleontol. 5, 215–247, 1980.
69 S. Krishnaswami, A. Mangini, J.H. Thomas, P. Sharma, J.K. Cochran, K.K. Turekian and P.D. Parker, ^{10}Be and ^{230}Th isotopes in manganese nodules and adjacent sediments: nodule growth histories and nuclide behavior, Earth Planet. Sci. Lett. 59, 217–234, 1982.
70 M. Kusakabe and T.L. Ku, Incorporation of Be isotopes and other trace metals into marine ferromanganese deposits, Geochim. Cosmochim. Acta 48, 2187–2193, 1984.
71 A. Mangini, M. Segl, H. Kudrass, M. Weidicke, G. Bonani, H.J. Hofmann, E. Morenzoni, M. Nessi, M. Suter and W. Wolfli, Diffusion and supply rates of ^{10}Be and ^{230}Th radioisotopes in two manganese encrustations from the South China Sea, Geochim. Cosmochim. Acta 50, 149–156, 1986.
72 T.L. Ku, Uranium series disequilibrium in deep sea sediments, 157 pp., Ph.D. Thesis, Columbia University, 1966.